

# A dense Pd/Ag membrane reactor for methanol steam reforming: Experimental study

Angelo Basile<sup>a,\*</sup>, Fausto Gallucci<sup>b</sup>, Luca Paturzo<sup>b</sup>

<sup>a</sup>*Institute on Membrane Technology, ITM-CNR, c/o University of Calabria, Via P. Bucci, Cubo 17/C, 87030 Rende (CS), Italy*

<sup>b</sup>*Department of Chemical Engineering and Materials, University of Calabria, Via P. Bucci, Cubo 42/A, 87030 Rende (CS), Italy*

Available online 12 May 2005

## Abstract

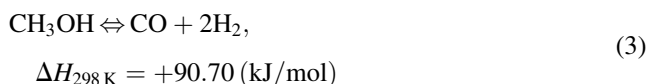
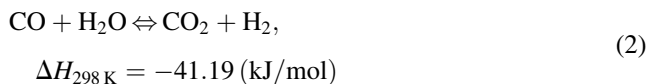
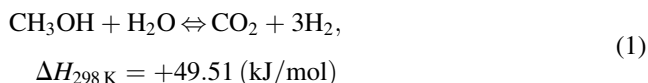
This paper focuses on an experimental study of the methanol steam reforming (MSR) reaction. A dense Pd/Ag membrane reactor (MR) has been used, and its behaviour has been compared to the performance of a traditional reactor (TR) packed with the same catalyst type and amount. The parameters investigated are reaction time, temperature, feed ratio and sweep gas flow rate. The few papers dealing with MR applications for the MSR reaction mainly analyse the effect of temperature and pressure on the reaction system. The investigation of new parameters permitted to better understand how the fluid-dynamics of the MR influences the hydrogen separation effect on methanol conversion and product selectivity. The comparison between MR and TR in terms of methanol conversion shows that the MR gives a higher performance than the TR at each operating condition investigated. Concerning hydrogen production, the experiments have shown that the overall selectivity towards hydrogen is identical for both MR and TR. However, the MR produces a free-CO hydrogen stream, which could be useful for direct application in proton exchange membrane fuel cells. A comparison, in terms of methanol conversion versus temperature, with literature data is also included.

© 2005 Elsevier B.V. All rights reserved.

**Keywords:** Methanol; Steam reforming; Hydrogen; Catalyst; Membrane reactor

## 1. Introduction

The methanol steam reforming (MSR) reaction is viewed as a very interesting and promising method for hydrogen production useful for fuel cell applications [1–4]. According to the literature, the chemical reactions considered are as follows:



Reactions (1) and (3) are both reversible and endothermic reactions and proceed under volume increase, suggesting that the highest methanol conversions are obtained at high temperature and low pressure. The exothermic reaction (2) is the so-called water gas-shift reaction which proceeds simultaneously with methanol steam reforming and without volume change.

However, this reaction when carried out in a traditional reactor leads to a hydrogen-containing mixture, so hydrogen needs purification before it can be fed to a polymer electrolyte membrane fuel cell (PEMFC). This separation is mainly devoted to remove CO which poisons the anodic catalyst of the fuel cell [1]. For this purpose, a fuel cell drive system based on methanol fuel consists of a methanol steam reformer and a gas cleaning unit which reduces the CO content of the hydrogen-rich gas and feeds the fuel cell. The reformer is equipped with a catalytic burner which provides the process heat to the reformer and converts all burnable gases in the flue gas into water and carbon dioxide. Recent studies concern the use of membrane reactors for methanol

\* Corresponding author. Tel.: +39 0984 492013; fax: +39 0984 402103.  
E-mail address: [a.basile@itm.cnr.it](mailto:a.basile@itm.cnr.it) (A. Basile).

steam reforming. The main advantage is to perform both reaction and pure hydrogen removal in the same device: in this way, it would be possible to replace the traditional system (reformer + gas cleaning unit) with the membrane reactor [1,5]. Furthermore, using steam as a sweep gas for hydrogen removal from the membrane reactor, the wet  $H_2$  stream could be directly suitable for the fuel cell. If compared to methanol and gasoline, among the fuel options for fuel cell vehicles, liquid hydrogen and compressed hydrogen (up to 34.5 MPa) are seen as the most advantageous ones [6]. However, hydrogen could require an unacceptably high infrastructure cost. Vice versa, infrastructure costs for liquid fuels (for example, methanol) should be sensitively lower. In this view, methanol steam reforming can be seen as a fuel source for producing hydrogen in situ at the local fuelling station [6].

The objective of this research work is to study from an experimental point of view the behaviour of a dense Pd/Ag membrane reactor (MR) in terms of methanol conversion as well as hydrogen and CO production in comparison with a traditional reactor (TR) operated at the same experimental conditions. Previous work in literature concerns this kind of reaction. Scientific works about traditional reactors are mainly focused on catalyst optimisation in order to reduce the CO content in the gaseous mixture coming out of the reactor [6–15]. This aspect is essential in order to avoid poisoning of the anodic catalyst in view of utilisation of the hydrogen-containing gas in the outlet stream as a feed for a PEMFC. However, to our knowledge, few scientific papers deal with membrane reactors applied to the methanol steam reforming reaction. These few papers [5,16–19] mainly analyse the effect of temperature and pressure on the reaction system. Pd [16,17], Pd/V/Pd, Pd<sub>75</sub>Ag<sub>25</sub>, Pd<sub>60</sub>Cu<sub>40</sub> [18] and Pd-supported [5,19] membranes were studied in the pressure range from 1 to 25 atm and at temperatures between 260 and 320 °C. The investigation of additional parameters could allow to understand better how the fluid-dynamics of the MR influences the hydrogen separation effect on methanol conversion and product selectivity. So the objective of this investigation is to perform a MR analysis focusing on the effect of other parameters, such as the  $H_2O/CH_3OH$  feed ratio and the sweep gas flow rate in addition to the reaction temperature. Moreover, an analysis of the performance over longer reaction times has been performed in order to check catalyst stability. A comparison with experimental data from literature is given in terms of  $CH_3OH$  conversion versus temperature.

## 2. Description of the process

### 2.1. Traditional and membrane reactor description

The TR consists of a stainless steel tube, length 25 cm, i.d. 0.67 cm, the reaction zone was 15 cm. The MR consists of a tubular stainless steel module, length 28 cm, i.d. 2 cm,

containing a pinhole-free Pd/Ag membrane permeable only to hydrogen, having a thickness of 50  $\mu m$ , o.d. 1.02 cm, length 15 cm. In particular, the dense membrane is welded to two stainless steel supports useful for the membrane housing. In the MR, catalyst pellets are packed in the membrane zone (15 cm length) thanks to glass spheres (2 mm diameter) placed into the stainless steel supports on both extremities of the membrane.

One graphite o-ring (99.53% C and 0.47% S) furnished by Gee Graphite Ltd. (England), 2.8 g, ensures that permeate and lumen streams do not mix with each other in the membrane module. The Pd/Ag membrane was produced by a lamination technique in E.N.E.A. Laboratories (Frascati, Italy); details of this technique have been presented elsewhere by Tosti et al. [20]. The upper temperature limit for the Pd/Ag membrane is 450 °C. The tubular membrane is plugged from one side, and reactants are fed by means of a stainless steel tube (o.d. 1/16 in., i.d. 1/40 in.) placed inside the membrane lumen; the end of this tube is at 1 cm from the plug of the membrane tube. In this way, reactants exit at the base of the catalyst bed, and both un-reacted and un-permeated species exit from the membrane tube lumen.

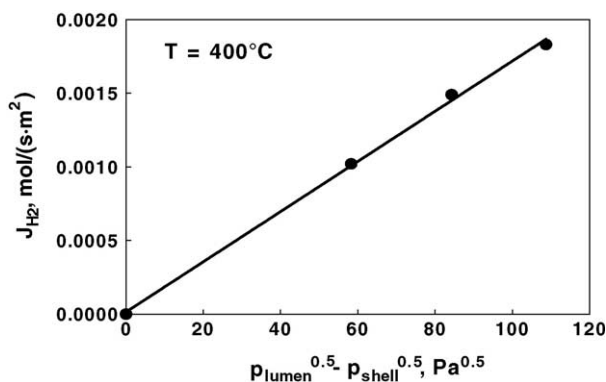


Fig. 1. Sievert plot for pure hydrogen permeation tests using the Pd/Ag membrane.  $T = 400$  °C.

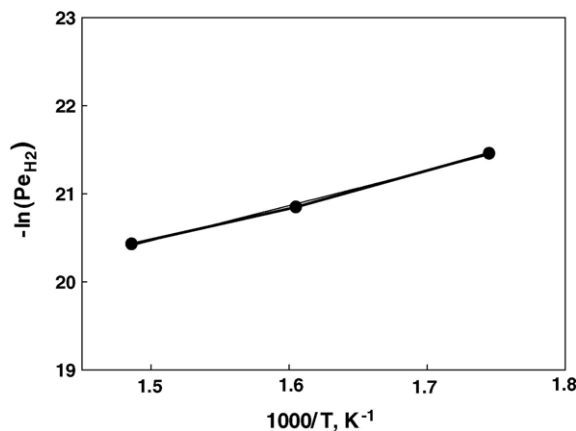


Fig. 2. Arrhenius plot for pure hydrogen permeation tests using the Pd/Ag membrane.  $E_a = 33.31$  kJ/mol,  $Pe_0 = 5.24 \times 10^{-7}$  mol  $m/(m^2 s Pa^{0.5})$ ,  $\Delta p = 0.4$  bar.

Table 1

Apparent activation energy and pre-exponential factor for hydrogen permeation through Pd/Ag membranes from the literature

$E_a$ (kJ/mol)	$Pe_0$ [ $10^{-5}$ mol m/(s m <sup>2</sup> kPa <sup>0.5</sup> )]	Reference
33.31	1.66	This work
48.50	9.33	Tosti et al. [20]
29.73	7.71	Basile et al. [21]
15.70	2.19	Koffler et al. [22]
15.50	2.54	Balovnev [23]
18.45	1.02	Itoh et al. [24]
12.48	0.38	Itoh and Xu [25]

## 2.2. Pure hydrogen permeation experiments

Figs. 1 and 2 show that both Sievert and Arrhenius laws, respectively, are followed. The apparent activation energy of hydrogen permeation,  $E_a$ , is 33.31 kJ/mol and the pre-exponential factor,  $Pe_0$ , is  $1.66 \times 10^{-5}$  mol m/(m<sup>2</sup> s kPa<sup>0.5</sup>). The temperature dependence of hydrogen permeability can be expressed by an Arrhenius-like expression, that becomes in our case:  $Pe = 1.66 \times 10^{-5} \exp(-4005/T)$ . The Pd/Ag membrane shows infinite permselectivity for hydrogen with respect to other gases. Table 1 shows a comparison of permeation parameters ( $E_a$  and  $Pe_0$ ) from different sources in literature. The parameters determined in this work are coherent with the experimental data found in literature.

## 2.3. Experimental details and description of the experimental plant

The reaction system was studied in terms of experimental tests. The reactor (TR or MR) was placed in a temperature-controlled proportional + integral + derivative control (P.I.D.) oven. The reaction temperature was in the range between 200 and 250 °C, while the permeation tests were conducted in the temperature range 300–400 °C. The inert carrier (N<sub>2</sub>) was fed by means of a mass-flow controller (Brooks Instruments 5850S) driven by a computer software furnished by Lira (Italy) for all experiments. H<sub>2</sub>O and CH<sub>3</sub>OH were fed by volumetric pumps (type FMQG6) furnished by General Control (Italy).

The total feed flow rate was set to  $1.17 \times 10^{-2}$  mol/min. Three different H<sub>2</sub>O/CH<sub>3</sub>OH feed gas ratios were also considered: 0.81, 1.22 and 2.43. These ratios were obtained by tuning the flow rates of CH<sub>3</sub>OH, H<sub>2</sub>O and N<sub>2</sub> carrier gas. The reaction pressure was held up at 1.25 bar by means of a regulating-valve system placed at the outlet side. For the MR, the permeate pressure was always 1 bar, and N<sub>2</sub> was used as sweep gas with a flow rate in the range between  $8.3 \times 10^{-4}$  and  $1.3 \times 10^{-2}$  mol/min. The same equipment was used for permeation tests. H<sub>2</sub>O and CH<sub>3</sub>OH liquid reactants were mixed and vaporised at 400 °C and then carried by the inert carrier gas into the reactor (both TR and MR). The outlet stream was completely condensed to remove the un-reacted H<sub>2</sub>O and CH<sub>3</sub>OH, and then the dry gaseous stream flow rate was measured by a bubble flow-

meter; its composition was detected using a temperature programmed HP 6890 gas chromatograph (GC) with a thermal conductivity detector (TCD) at 250 °C and He as carrier gas. The GC is equipped with three packed columns: Porapack R 50/80 (8 ft × 1/8 in.) and Carboxen<sup>TM</sup> 1000 (15 ft × 1/8 in.) connected in series, Molecular Sieve 5 Å (6 ft × 1/8 in.). A 10-way valve was used to optimise the total time of analysis which was about 5.1 min, the analysis procedure was controlled by a software developed by Hewlett-Packard. For the MR, which has two outlet streams (permeate and retentate), two TCD detectors were simultaneously used for measuring the composition at the same time.

Both TR and MR were packed with 7.5 g of a CuO (51%)/ZnO (31%)/Al<sub>2</sub>O<sub>3</sub> (18%) commercial catalyst (type ICI 83-3, size 250–450 μm) furnished by Syntex. Before reaction, the catalyst was pre-heated using N<sub>2</sub> at 180 °C under atmospheric pressure, and afterwards reduced using a mixture of N<sub>2</sub>–H<sub>2</sub> (1.5% H<sub>2</sub>) at the same temperature for 24 h. The overall reaction time was 5 h for both MR and TR.

A flat temperature profile along the reactor during the reaction has been achieved by using a heating system connected to a four point thermocouple inserted into the lumen for both TR and MR.

## 3. Results and discussion

The following definitions are used for describing the performance of the TR and MR:

$$\text{CH}_3\text{OH conversion}(X_{\text{CH}_3\text{OH}}, \%) = \frac{\text{CO}_{\text{out}} + \text{CO}_{2,\text{out}}}{\text{CH}_3\text{OH}_{\text{in}}} \times 100 \quad (4)$$

$$\text{H}_2 \text{ selectivity}(S_{\text{H}_2}, \%) = \frac{\text{H}_{2,\text{out}}}{\text{H}_{2,\text{out}} + \text{CO}_{\text{out}} + \text{CO}_{2,\text{out}}} \times 100 \quad (5)$$

$$\text{CO selectivity}(S_{\text{CO}}, \%) = \frac{\text{CO}_{\text{out}}}{\text{H}_{2,\text{out}} + \text{CO}_{\text{out}} + \text{CO}_{2,\text{out}}} \times 100 \quad (6)$$

$$\text{CO}_2 \text{ selectivity}(S_{\text{CO}_2}, \%) = \frac{\text{CO}_{2,\text{out}}}{\text{H}_{2,\text{out}} + \text{CO}_{\text{out}} + \text{CO}_{2,\text{out}}} \times 100 \quad (7)$$

The subscript “out” indicates the total outlet flow rate of each species. In particular, for the TR, only one outlet stream is present for each species, while for the MR, two outlet streams are present only for hydrogen, because the dense Pd/Ag membrane exhibits infinite permselectivity for H<sub>2</sub>.

Figs. 3 and 4 show the CH<sub>3</sub>OH conversion versus time of reaction at three different temperatures, 200, 220 and 250 °C, for the TR and the MR, respectively. Both figures

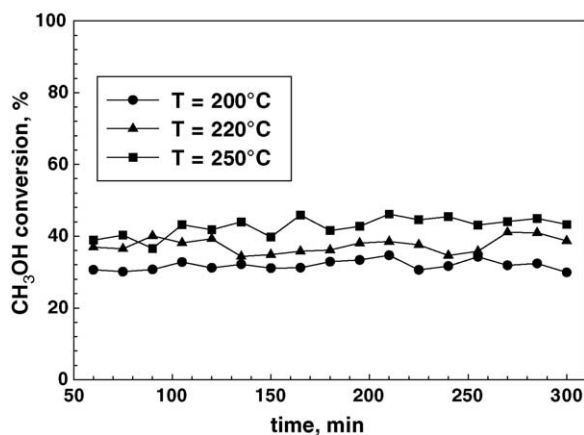


Fig. 3. CH<sub>3</sub>OH conversion vs. time for the TR at different temperatures. H<sub>2</sub>O/CH<sub>3</sub>OH = 1.22,  $p = 1.25$  bar.

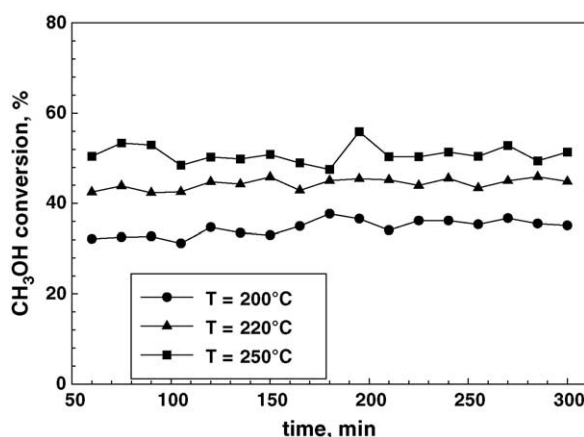


Fig. 4. CH<sub>3</sub>OH conversion vs. time for the MR at different temperatures. H<sub>2</sub>O/CH<sub>3</sub>OH = 1.22,  $p_{\text{lumen}} = 1.25$  bar,  $p_{\text{shell}} = 1.00$  bar, sweep gas flow rate =  $8.3 \times 10^{-4}$  mol/min.

show a quite constant trend over time at each temperature investigated; moreover, according to the endothermicity of the overall reaction system, CH<sub>3</sub>OH conversion increases with temperature at fixed reaction time. For example, at 225 min of reaction time, CH<sub>3</sub>OH conversion for the TR is 30.6, 37.59 and 44.57% at 200, 220 and 250 °C, respectively (cf. Fig. 3). With regard to the MR, CH<sub>3</sub>OH conversion is always higher with respect to the TR; in fact, at the same reaction time of 225 min, CH<sub>3</sub>OH conversion is 36.17, 43.95 and 50.3% at 200, 220 and 250 °C, respectively (cf. Fig. 4). Experimental results regarding long-term experiments are not reported in the paper; however, the Pd/Ag membrane has been used for more than two months without any sign of damage. The difference in the behaviour of the TR and the MR is attributed to H<sub>2</sub> removal obtained in the MR. Considering the quite constant trend during 5 h, an average value of CH<sub>3</sub>OH conversion has been calculated at each temperature for both TR and MR. Both are compared in Fig. 5: the higher CH<sub>3</sub>OH conversion of the MR is evident. The difference between TR and MR increases with temperature, due to the increase of hydrogen permeability

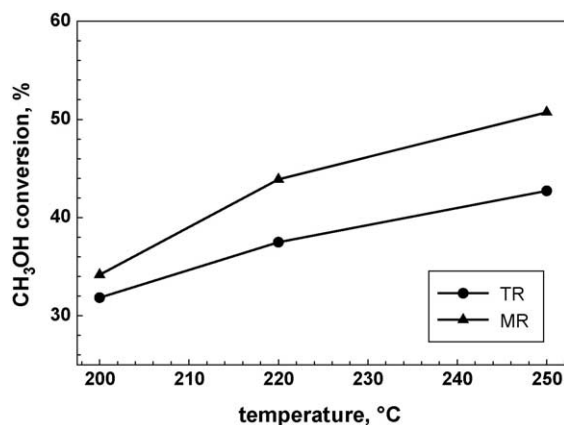


Fig. 5. CH<sub>3</sub>OH conversion (average values) vs. temperature for TR and MR. H<sub>2</sub>O/CH<sub>3</sub>OH = 1.22,  $p_{\text{lumen}} = 1.25$  bar,  $p_{\text{shell}} = 1.00$  bar, sweep gas flow rate =  $8.3 \times 10^{-4}$  mol/min (for MR).

Table 2

Reaction tests for the TR: average values calculated over 5 h of reaction time

	Temperature (°C)		
	200	220	250
CH <sub>3</sub> OH conversion (% , average)	31.84	37.49	42.72
H <sub>2</sub> selectivity (% , average)	82.33	83.68	81.36
CO selectivity (% , average)	0.08	0.25	0.62
CO <sub>2</sub> selectivity (% , average)	17.59	16.07	18.02

H<sub>2</sub>O/CH<sub>3</sub>OH = 1.22;  $p = 1.25$  bar.

with temperature according to the Arrhenius-like expression (see Section 2.2). For example, at 200 °C, CH<sub>3</sub>OH conversion (average value) is about 32% for the TR versus about 35% for the MR, while at 250 °C, CH<sub>3</sub>OH conversion (average value) is about 43% for the TR versus about 51% for the MR. More in detail, Tables 2 and 3 give average values of CH<sub>3</sub>OH conversion and product (H<sub>2</sub>, CO and CO<sub>2</sub>) selectivity achieved during 5 h of reaction time for TR and MR, respectively. In particular, CO selectivity increases with temperature for both reactors; for example, it is 0.08% at 200 °C and 0.62% at 250 °C for the TR, versus 0.05% at 200 °C and 0.47% at 250 °C for the MR. The increasing CO selectivity with temperature can be explained considering the reactions cited in Section 1, specifically reactions (2) and (3). Reaction (2) is exothermic, while reaction (3) is endothermic, so that increasing temperature reaction (2)

Table 3

Reaction tests for the MR: average values calculated over 5 h of reaction time

	Temperature (°C)		
	200	220	250
CH <sub>3</sub> OH conversion (% , average)	34.58	44.3	50.83
H <sub>2</sub> selectivity (% , average)	80.67	83.45	82.84
CO selectivity (% , average)	0.05	0.11	0.47
CO <sub>2</sub> selectivity (% , average)	19.29	16.44	16.68

H<sub>2</sub>O/CH<sub>3</sub>OH = 1.22;  $p = 1.25$  bar.

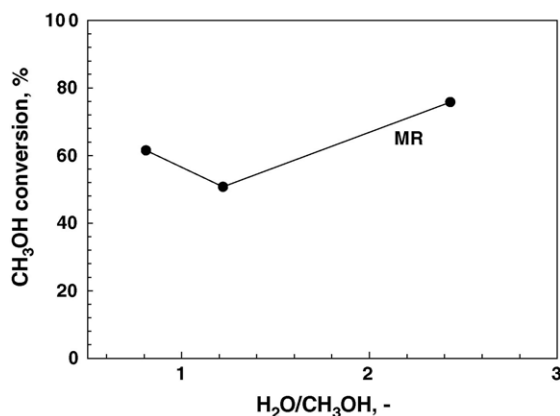


Fig. 6. CH<sub>3</sub>OH conversion vs. H<sub>2</sub>O/CH<sub>3</sub>OH feed ratio for the MR.  $T = 250\text{ }^{\circ}\text{C}$ ,  $p_{\text{lumen}} = 1.25\text{ bar}$ ,  $p_{\text{shell}} = 1.00\text{ bar}$ , sweep gas flow rate ( $Q_{\text{sweep gas}}$ ) =  $8.3 \times 10^{-4}\text{ mol/min}$ ,  $Q_{\text{TOT}} = 1.17 \times 10^{-2}\text{ mol/min}$ .

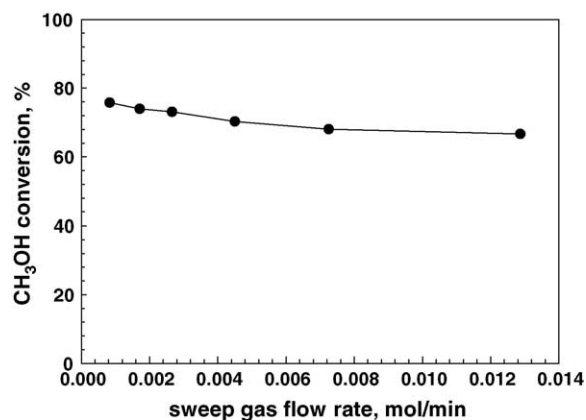


Fig. 7. CH<sub>3</sub>OH conversion vs. sweep gas flow rate for the MR. H<sub>2</sub>O/CH<sub>3</sub>OH = 2.43,  $T = 250\text{ }^{\circ}\text{C}$ ,  $p_{\text{lumen}} = 1.25\text{ bar}$ ,  $p_{\text{shell}} = 1.00\text{ bar}$ .

(which consumes CO) is disfavoured while reaction (3) (which produces CO) is favoured. However, CO selectivity decreases changing from the TR to the MR. Since the only difference between the two reactors is the presence of the membrane, this evidence can be discussed considering again reactions (2) and (3) cited in Section 1. Reaction (2) consumes 1 mol of CO per mole of H<sub>2</sub> removed (through the membrane), while reaction (3) produces half a mole of CO per mole of H<sub>2</sub> removed: under these conditions, there is a net consumption of CO so that CO selectivity decreases.

An unclear behaviour was found for both H<sub>2</sub> and CO<sub>2</sub> selectivity, although their values are similar at each temperature investigated, probably due to a different and not predictable contribution of each reaction considered in Section 1.

Fig. 6 shows the behaviour of CH<sub>3</sub>OH conversion versus H<sub>2</sub>O/CH<sub>3</sub>OH feed ratio at 250 °C for the MR. CH<sub>3</sub>OH conversion presents a minimum at a H<sub>2</sub>O/CH<sub>3</sub>OH feed ratio of 1.25 where it reaches about 51%. Anyway, the highest value of H<sub>2</sub>O/CH<sub>3</sub>OH feed ratio gives the highest CH<sub>3</sub>OH conversion: in fact, it is about 76% at a H<sub>2</sub>O/CH<sub>3</sub>OH feed ratio of 2.43.

When increasing the sweep gas flow rate, CH<sub>3</sub>OH conversion seems to tend to a constant value of about 67%, reached at a sweep gas flow rate of  $1.3 \times 10^{-2}\text{ mol/min}$ , as shown in Fig. 7. In literature, it is well known that reactant conversion increases with increasing sweep gas flow rate, until a *plateau* is reached, for example, in the methane partial oxidation reaction [21]. In the case of this work, however, CH<sub>3</sub>OH conversion seems to exhibit a slightly decreasing trend. It should be noted here that these reaction tests have been carried out consecutively, so that the last experimental point was measured after 20 h of reaction time. The reason of this trend is probably due to carbon deposition during long-term experiments. In fact, carbon deposition is the main problem of methanol steam reforming carried out over Cu-containing catalysts [3]. Moreover, long-term (20 h) experiments carried out using the TR gave an amount

of 0.117 g of carbon deposited on the catalyst surface. This carbon amount has been determined by feeding pure oxygen (106 ml/min) at 550 °C after the reaction test, and by analysing the outlet stream for C-containing gases (CO and CO<sub>2</sub>). For the MR, in order to avoid membrane cracking, the same experimental test for detection of carbon deposition has not been performed. Another aspect to be taken into account and related to the behaviour shown in Fig. 7 is the kind of control mechanism that takes place. In this case, probably, kinetic control of the reaction system prevails. This means that the hydrogen production rate is less than the hydrogen removal rate, so an increase in the sweep gas flow rate (i.e. increasing the hydrogen removal rate) cannot give a benefit in terms of higher reactant conversion. Finally, Fig. 7 shows that, for our experimental set of parameters, the sweep gas flow rate is not a salient variable to be taken into account.

Fig. 8 shows a comparison of CH<sub>3</sub>OH conversion versus temperature with literature data. Some experimental details are reported in Table 4. A general increasing trend is seen. The different behaviour of each cited work is certainly due to the different operating conditions adopted by each author

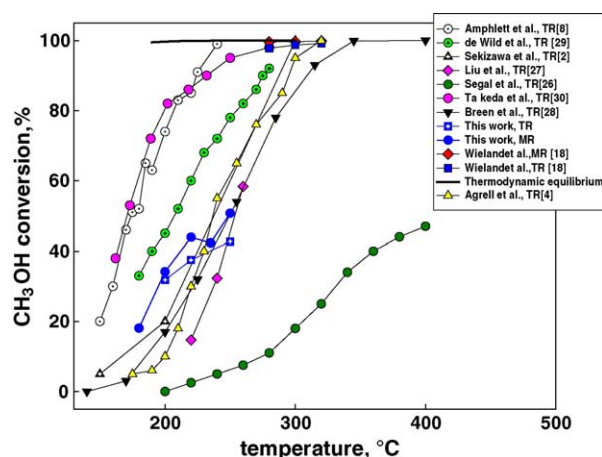


Fig. 8. CH<sub>3</sub>OH conversion vs. temperature: comparison with literature data.

Table 4  
Methanol steam reforming: operating conditions found in literature

Authors	<i>p</i> (atm)	Carrier gas	H <sub>2</sub> O/CH <sub>3</sub> OH	Catalyst	
				Type	Weight (g)
Sekizawa et al. [2]	1	N <sub>2</sub>	3–5	Cu/ZnO/Al <sub>2</sub> O <sub>3</sub>	–
Agrell et al. [4]	1	N <sub>2</sub>	1.3	Cu/ZnO/Al <sub>2</sub> O <sub>3</sub> (G-6MR)	0.05
Amphlett et al. [8]	1	–	1	Cu/ZnO/Al <sub>2</sub> O <sub>3</sub> (C18HC)	1–6.5
Wieland et al. [18], TR	25	–	–	Cu/ZnO/Al <sub>2</sub> O <sub>3</sub>	–
Wieland et al. [18], MR	25	–	–	Cu/ZnO/Al <sub>2</sub> O <sub>3</sub>	–
Segal et al. [26]	1	N <sub>2</sub>	1	Cu/Al (LDH)	0.15
Liu et al. [27]	1	N <sub>2</sub>	1	Cu/CeO <sub>2</sub>	0.3
Breen and Ross [28]	1	–	1.3	Cu-based	0.1
de Wild and Verhaak [29]	1.3–1.5	N <sub>2</sub>	1.5–2	Cu-based	74
Takeda et al. [30]	1	N <sub>2</sub>	1.5	Cu/ZnO/Al <sub>2</sub> O <sub>3</sub> + Ru/Al <sub>2</sub> O <sub>3</sub>	–
This work	1.25	N <sub>2</sub>	1.22	Cu/ZnO/Al <sub>2</sub> O <sub>3</sub> (ICI 83-3)	7.5

(see Table 4), but the MR should give higher CH<sub>3</sub>OH conversion than the TR if operated at the same experimental conditions. In principle, from an economical point of view, the MR should permit to achieve the same conversion as the TR using a lower amount of catalyst, and this implies a reduction of the catalyst cost for a MR-equipped plant. On the other hand, the TR produces an impure H<sub>2</sub> stream that requires a separation unit which adds to the cost for a TR-equipped plant (while the dense MR is able to produce a pure H<sub>2</sub> stream). The operating conditions must be properly tuned to get an optimum of the economical potential of a certain plant, either TR- or MR-equipped. Certainly, the optimum set of these parameters is different changing from TR to MR, and the economical optimum of the overall plant should also be compatible with realistic operating conditions that would allow to achieve energy savings. However, this is not the subject of this paper.

#### 4. Conclusions

The methanol steam reforming reaction has been studied both in a TR and a MR, from an experimental viewpoint. This study confirms the potential of the membrane reactor for increasing the conversion over that of a traditional system, operated at the same experimental conditions. By using the MR, it is possible to easily separate H<sub>2</sub> from all the other gases (including CO) in order to have a CO-free H<sub>2</sub> stream for direct utilisation in a polymer electrolyte membrane fuel cell. Moreover, in the MR, the CO selectivity is lower than in the TR.

The CH<sub>3</sub>OH conversion has been monitored by changing several reaction parameters, such as the H<sub>2</sub>O/CH<sub>3</sub>OH feed ratio, the reaction temperature and the sweep gas flow rate during 5 h of reaction time.

In particular, the main results of this work can be summarized as stated below:

- (1) No significant variation of catalytic activity has been observed within the range of the reaction time investigated. In fact, for example, CH<sub>3</sub>OH conversion

maintained around 43% in the TR and 51% in the MR operated at 250 °C, 1.25 bar and a H<sub>2</sub>O/CH<sub>3</sub>OH feed ratio of 1.22.

- (2) For the MR, CH<sub>3</sub>OH conversion increases with increasing H<sub>2</sub>O/CH<sub>3</sub>OH feed ratio, but passes through a minimum of 51% at a H<sub>2</sub>O/CH<sub>3</sub>OH feed ratio of 1.22. A maximum CH<sub>3</sub>OH conversion of 76% has been achieved at a H<sub>2</sub>O/CH<sub>3</sub>OH feed ratio of 2.43.
- (3) The increase of the sweep gas flow rate from  $8.3 \times 10^{-4}$  to  $1.3 \times 10^{-2}$  mol/min does not produce an increase of CH<sub>3</sub>OH conversion, which shows a *plateau* of about 67%.
- (4) According to the endothermicity of the overall reaction system, CH<sub>3</sub>OH conversion (average value) increases with temperature for both the MR and the TR, and the MR overcomes the TR at each temperature investigated.
- (5) With regard to reaction selectivity, the hydrogen selectivity is quite high (around 80%) for both the TR and the MR. However, CO selectivity is lower in the MR than in the TR at each temperature investigated.

#### Acknowledgements

The authors wish to thank Syntex for furnishing the catalyst. The authors appreciate and thank Eng. S. Fragale for performing some experiments concerning the TR and the MR.

#### References

- [1] J. Han, I.-S. Kim, K.-S. Choi, J. Power Sources 86 (2000) 223–227.
- [2] K. Sekizawa, S. Yano, K. Eguchi, H. Arai, Appl. Catal. A: Gen. 169 (1998) 291–297.
- [3] T. Takahashi, M. Inoue, T. Kai, Appl. Catal. A: Gen. 218 (2001) 189–195.
- [4] J. Agrell, H. Birgersson, M. Boutonnet, J. Power Sources 106 (1–2) (2002) 249–257.
- [5] Y.-M. Lin, M.-H. Rei, Catal. Today 67 (2001) 77–84.
- [6] J.C. Amphlett, M.J. Evans, R.A. Jones, R.F. Mann, R.D. Weir, Can. J. Chem. Eng. 59 (1981) 720–727.

- [7] J.C. Amphlett, M.J. Evans, R.F. Mann, R.D. Weir, *Can. J. Chem. Eng.* 63 (1985) 605–611.
- [8] J.C. Amphlett, R.F. Mann, R.D. Weir, *Can. J. Chem. Eng.* 66 (1988) 950–956.
- [9] J.C. Amphlett, R.F. Mann, B.A. Peppley, in: H.E. Curry-Hyde, R.F. Howe (Eds.), *Stud. Surf. Sci. Catal.*, vol. 81, Elsevier, Amsterdam, 1994, ISBN: 0-444-89535-3, pp. 409–412.
- [10] R. Dümpelmann, Ph.D. Thesis, Eidgenössischen Technischen Hochschule, Zürich, Switzerland, 1992, cited reference in M. Schuessler, O. Lamla, T. Stefanovsky, C. Klein, D. zur Megede, Autothermal reforming of methanol in an isothermal reactor—concept and realisation, *Chem. Eng. Technol.* 24 (11) (2001) 1141–1145.
- [11] C.J. Jiang, D.L. Trimm, M.S. Wainwright, N.W. Cant, *Appl. Catal. A: Gen.* 93 (2) (1993) 245–255.
- [12] C.J. Jiang, D.L. Trimm, M.S. Wainwright, N.W. Cant, *Appl. Catal. A: Gen.* 97 (2) (1993) 145–158.
- [13] B.A. Peppley, Ph.D. Thesis, RMC Kingston, Ont., Canada, 1997, cited reference in M. Schuessler, O. Lamla, T. Stefanovsky, C. Klein, D. zur Megede, Autothermal reforming of methanol in an isothermal reactor—concept and realisation, *Chem. Eng. Technol.* 24 (11) (2001) 1141–1145.
- [14] B.A. Peppley, J.C. Amphlett, L.M. Kearns, R.F. Mann, *Appl. Catal. A: Gen.* 179 (1–2) (1999) 21–29.
- [15] B.A. Peppley, J.C. Amphlett, L.M. Kearns, R.F. Mann, *Appl. Catal. A: Gen.* 179 (1999) 31–49.
- [16] B. Emonts, J.B. Hansen, H. Schmidt, T. Grube, B. Höhle, R. Peters, A. Tschauder, *J. Power Sources* 86 (1–2) (2000) 228–236.
- [17] R.E. Buxbaum, *Sep. Sci. Technol.* 34 (1999) 2113–2123.
- [18] S. Wieland, T. Melin, A. Lamm, *Chem. Eng. Sci.* 57 (9) (2002) 1571–1576.
- [19] Y.-M. Lin, M.-H. Rei, *Int. J. Hydrogen Energy* 25 (2000) 211–219.
- [20] S. Tosti, L. Bettinali, V. Violante, A. Basile, M. Chiappetta, A. Criscuoli, E. Drioli, C. Rizzello, in: *Proceedings of the 20th Symposium on Fusion Technology*, Marseille, France, September 7–11, 1998, pp. 1033–1036.
- [21] A. Basile, L. Paturzo, F. Laganà, *Catal. Today* 67 (2001) 65–75.
- [22] S.A. Koffler, J.B. Hudson, G.S. Ansell, *Trans. AIME* 245 (1969) 1735–1740.
- [23] Yu.A. Balovnev, *Russ. J. Phys. Chem.* 48 (1974) 409–410.
- [24] N. Itoh, W.-C. Xu, K. Haraya, *J. Membr. Sci.* 56 (1991) 315–325.
- [25] N. Itoh, W.-C. Xu, *Appl. Catal. A: Gen.* 107 (1993) 83–100.
- [26] S.R. Segal, K.B. Anderson, K.A. Carrado, C.L. Marshall, *Appl. Catal. A: Gen.* 231 (2002) 215–226.
- [27] Y. Liu, T. Hayakawa, K. Suzuki, S. Hamakawa, T. Tsunoda, T. Ishii, M. Kumagai, *Appl. Catal. A: Gen.* 223 (2002) 137–145.
- [28] J.P. Breen, J.R.H. Ross, *Catal. Today* 51 (3–4) (1999) 521–533.
- [29] P.J. de Wild, M.J.F.M. Verhaak, *Catal. Today* 60 (1–2) (2000) 3–10.
- [30] K. Takeda, A. Baba, Y. Hishinuma, T. Chikahisa, *JSAE Rev.* 23 (2002) 183–188.